Nanotechnology **19** (2008) 465301 (9pp) doi:10.1088/0957-4484/19/46/465301

Controlling the surface properties of nanostructures for studies of polymerases

Aurélien Crut[1], **Daniel A Koster**[2], **Zhuangxiong Huang, Susanne Hage and Nynke H Dekker**[3]

Kavli Institute of Nanoscience, Faculty of Applied Sciences, Delft University of Technology, Lorentzweg 1, 2628 CJ Delft, The Netherlands

E-mail: n.h.dekker@tudelft.nl

Received 27 June 2008, in final form 2 September 2008
Published 21 October 2008
Online at stacks.iop.org/Nano/19/465301

Abstract

We report the successful functionalization of optically accessible nanostructures, suitable for single-molecule experiments at physiological substrate concentrations, with polyethylene glycol. Characterization of the coating in terms of roughness, protein repellence, and specific immobilization of DNA is described. We present an application of this technique in the detection of polymerase activity within nanostructures, which demonstrates the opportunities made possible through the integration of nanofabricated structures with surface functionalization.

S Supplementary data are available from stacks.iop.org/Nano/19/465301

1. Introduction

Single-molecule studies of DNA and RNA polymerases have developed rapidly in recent years [1–6]. Two main motivations underlie these experiments: on the one hand, the large biological importance of these enzymes involved in DNA replication and transcription, and, on the other hand, the fact that these measurements could provide an efficient way to sequence DNA [4, 6].

Among the various techniques proposed to study polymerase activity in real time and at the single-molecule level, fluorescence-based methods currently appear most promising [2, 4], and directly observing the successive incorporation of fluorescent nucleotides would be of particular interest. However, these experiments depend on the fulfillment of two main requirements. First, either DNA molecules or polymerases should be immobilized, preferably in a well-controlled manner, and the immobilization scheme should have a minimal impact on polymerization. Second, the illumination conditions should allow for the observation of single incorporation events in the presence of micromolar concentrations of nucleotides, which are required for optimal enzymatic activity [7]. This second condition is not accessible in conventional fluorescence microscopy, due to the fundamental lower limit that diffraction places on the size of a light beam, and therefore on the distance over which two individual fluorophores can be resolved. This limitation restricts the range of application of single-molecule studies to situations involving concentrations of fluorescent species in the nanomolar range.

Fortunately, various novel techniques have recently been developed to circumvent this limitation of conventional far-field techniques, primarily by achieving smaller observation volumes. Examples include the direct control of the size of the illuminating light beam, as in near-field scanning optical microscopy (NSOM) [8, 9], or the use of nanostructures which define small observation volumes. In particular, it has been shown that an adequate solution to the aforementioned issue is provided by nanocavities drilled in a metallic layer, referred to as 'zero-mode waveguides'. Indeed, when their lateral size is sufficiently small (typically below the wavelength of the light used for illumination), the use of zero-mode waveguides leads to a dramatic decrease of the observation volume compared with far-field techniques, down to zeptoliter (10^{-21} L) scales [10, 11]. In addition to the resulting possibility of using high concentrations of fluorescent

[1] Present address: Laboratoire de Spectrométrie Ionique et Moléculaire, Université Claude Bernard Lyon 1, 43 boulevard du 11 Novembre 1918, 69622 Villeurbanne cedex, France.

[2] Present address: Departments of Physics of Complex Systems and Molecular Cell Biology, Weizmann Institute of Science, Rehovot, 76100, Israel.

[3] Author to whom any correspondence should be addressed.

molecules, zero-mode waveguides present another important advantage, namely the short residency time of molecules diffusing in the observation volume. This facilitates the distinction between the timescales associated to diffusion and to biological processes, respectively [10].

In the pioneering work that introduced zero-mode waveguides [10], uncoated waveguides were employed: polymerases were immobilized in zero-mode waveguides by non-specific binding to glass surfaces. While the authors observed reasonable activity from the surface-bound polymerases, their approach has potential drawbacks since it induces the general risk of highly undesirable non-specific interactions between the biomolecules under study and the surfaces, and may lead to a partial or total loss of their activity. Therefore, the development of surface coating strategies for waveguides is desirable. The ideal surface coating should present three key features. First, the chemicals deposited should form a stable, thin, and flat layer, these two last requirements having a special importance in the context of nanostructure coating, as the space available in this context is severely restricted. Second, the surface coating should prevent undesirable non-specific interactions between biomolecules and surfaces. Finally, the surface should still allow for the immobilization of the biomolecules to be studied, if possible through a specific binding and with a tunable density.

Here, we report on the development of an alternative approach based on the specific attachment of DNA templates in the waveguides using polyethylene glycol (PEG), a polymer which has been successfully used for applications such as studies of cell adhesion [12] and single-molecule fluorescence energy transfer (FRET) [13, 14]. We first describe the coating of glass surfaces with PEG, and provide an extensive characterization of these surfaces in terms of roughness, protein and nucleotide repellence, and specific attachment of DNA. Next, the successful extension of the coating procedure to nanostructures is demonstrated. For both glass surfaces and nanostructures, we demonstrate the power of atomic force microscopy (AFM) as a characterization tool. Finally, we present results that demonstrate the incorporation of fluorescent nucleotides by polymerases within PEG-coated nanostructures (including zero-mode waveguides) and open the way to real-time measurements.

2. Properties of PEG-coated surfaces

We first briefly describe the coating procedure employed (further details are available in the supporting information, available at stacks.iop.org/Nano/19/465301). PEG-coated surfaces were typically obtained in three steps. First, standard microscope glass slides were extensively cleaned by successive sonications in 1% Alconox (Sigma) and in pure ethanol, followed by treatment in an oxygen plasma (Structure Probe). Then, the slides were reacted with 1% aminosilane (Vectabond, Brunschwig Chemie) in acetone. Finally, freshly made dilutions in water of non-biotinylated PEG (20% w/v, M-PEG-SPA, MW 5000, Nektar Therapeutics) and biotinylated PEG (concentration dependent on the application, Biotin-PEG-NHS, MW 3400, Nektar Therapeutics), were incubated on the slides.

To verify that the PEG coating does not lead to a dramatic increase in surface roughness, which would be detrimental to optical experiments, we compared the roughness of untreated glass slides and PEG-coated glass slides in air by AFM. Following thorough cleaning, glass slides displayed a peak-to-peak roughness smaller than 1 nm (with the exception of a few holes that were systematically observed in AFM images) (figure 1(a)). We observed only a minor increase in surface roughness as a result of the PEGylation procedure: the roughness remained below 1 nm (figure 1(b)). Since the PEG molecules themselves are not directly observed by AFM, one could argue that the modest roughness variation could be attributable to a lack of coating. However, we observed that such slides exhibited very different properties in terms of biomolecule adsorption (see below), attesting to a profound modification of their surface chemistry. Therefore, our observations are fully consistent with the presence of a regular layer of PEG on the surface.

We then investigated the ability of our PEG-coated surfaces to prevent the non-specific adsorption of various enzymes, including DNA polymerases. Again using AFM as an imaging tool, we compared the adsorption of solutions of Sequenase and Klenow polymerases in 1 μm^2 regions, after temporary incubation on top of untreated and PEG-coated glass surfaces. We observed that both Sequenase (figure 1(d)) and Klenow (data not shown) do not adsorb on PEG-coated surfaces, whereas, in otherwise similar conditions, they densely bind to untreated glass surfaces (figure 1(c)). Similar behavior was observed for other proteins such as streptavidin and bovine serum albumin (BSA). Among the proteins we tested, only lyzosyme was not efficiently repelled by our PEG surfaces, presumably a consequence of its much smaller size.

Since the observation of nucleotide incorporation by polymerases requires a low non-specific adsorption not only of polymerases, but also of labeled nucleotides, we tested how various fluorescently labeled nucleotides interacted with PEG-coated surfaces. To quantify this interaction, fluorescence microscopy was preferred to AFM as an imaging tool, since direct observation by AFM is prohibited by the small size of nucleotides, while their fluorescent labeling permits optical visualization. Interestingly, we did not observe universal behavior among the different types of labeled nucleotides that we tested. On the one hand, figures 1(e) and (f) convincingly show that PEG surfaces efficiently repel gamma-phosphate-labeled nucleotides (in which the fluorophore is attached to the phosphate group of the nucleotide), which represent promising nucleotides for DNA sequencing [15]. On the other hand, we observed that standard base-labeled nucleotides (in which the fluorophore is attached to the base) yield a much larger adsorption on PEG-coated surfaces (figure S2 (available at stacks.iop.org/Nano/19/465301)). This would appear to preclude the monitoring of polymerase activity via base-labeled nucleotides; however, we observed that this problem can be largely circumvented by a preliminary passivation step involving the adsorption of unlabeled nucleotides on the slide prior to the incubation of fluorescent ones, reducing the non-specific adsorption to densities below 1 fluorophore μm^{-2} (figure S2b (available at stacks.iop.org/Nano/19/465301)).

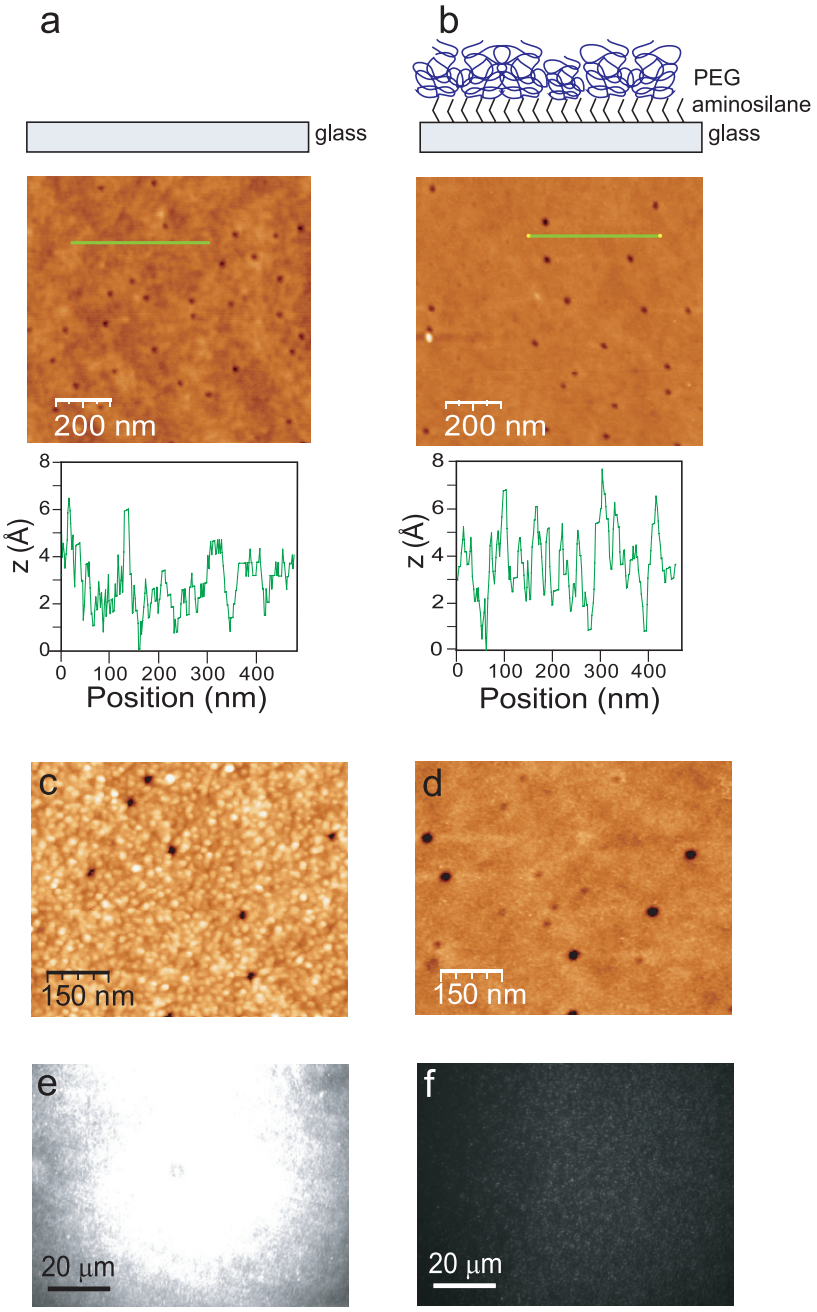

Figure 1. Main features of bare and PEG-coated glass surfaces. (a) Topography of a glass slide before coating. The image was obtained by AFM (in air). The glass surface includes localized depressions (black dots in the image). Leaving aside these depressions, the peak-to-peak roughness is of the order of a few angstroms. (b) Topography after PEGylation (with pure non-biotinylated PEG). The peak-to-peak roughness increases only slightly and remains smaller than 1 nm. ((c), (d)) Adsorption of Sequenase on bare and PEG-coated glass surfaces. 50 μL of commercial Sequenase (GE Healthcare, diluted 20 times in PBS) were incubated for 30 min on a clean, uncoated glass slide (c) and on a slide coated with non-biotinylated PEG (d). AFM images taken after rinsing the two slides reveal a dramatically different behavior: whereas the glass surface is densely covered with proteins, the PEG slide remains essentially free of bound proteins. ((e), (f)) Adsorption of labeled nucleotides on glass and PEG-coated slides. A solution of gamma-phosphate-labeled nucleotides (TAMRA-dATP) at 1 μM concentration was incubated for 5 min on a clean, uncoated glass slide (e) and on a slide coated with non-biotinylated PEG (f). Fluorescence images taken after rinsing the two slides show that nucleotides have adsorbed densely on the glass surface; in contrast, the PEG-coated slide displays only weak coverage ($<$1 spot μm^{-2}).

Finally, the surface passivation in our experiments must be compatible with the immobilization of specific biomolecules such as DNA. The use of biotin–streptavidin chemistry constitutes a standard approach to attach DNA to surfaces, since it ensures a stable and specific binding of DNA. Fortunately, it is compatible with PEGylation, since a controlled fraction of the PEG molecules employed can be biotinylated. This strategy allows the subsequent attachment of streptavidin, followed by the specific attachment of biotinylated biomolecules to the surface [13]. We

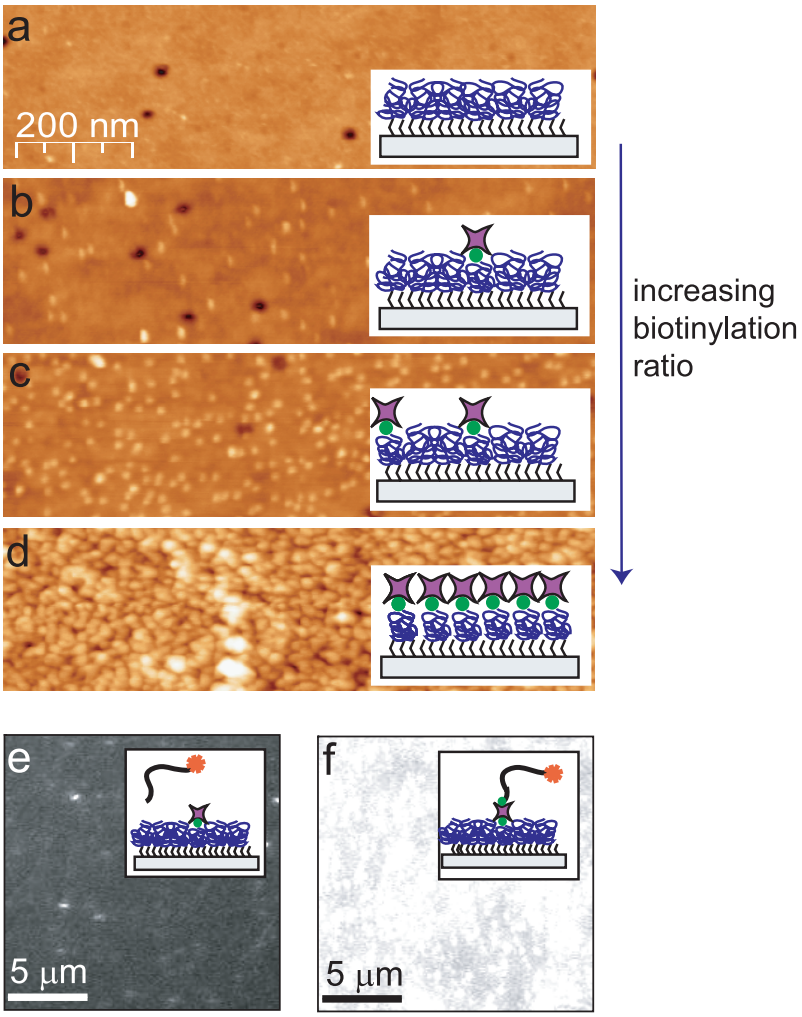

Figure 2. Specific, streptavidin-mediated attachment of biotinylated DNA onto PEG surfaces. ((a)–(d)) Demonstration of tunable streptavidin adsorption. A 0.1 mg ml^{-1} streptavidin solution was incubated on slides PEGylated with (a) 0%, (b) 0.5%, (c) 5% and (d) 33% fractions of biotinylated PEG, respectively. The AFM pictures of the slide after coating with streptavidin are shown. Individual streptavidin molecules appear as higher-lying yellow dots in these images. Their density clearly increases with the degree of biotinylation, from an almost null adsorption in (a) to a dense coverage of the slide in (d). The insets represent a schematic view of the slide surface. ((e) and (f)) Specificity of DNA attachment on a PEG-coated glass slide. The specific and non-specific adsorptions of DNA were measured using fluorescence microscopy. The surface used for this test was a glass slide coated with partly biotinylated PEG (PEGylation performed with 20% w/v non-biotinylated PEG and 0.01% w/v biotinylated PEG). The adsorptions of 1 μM solutions of a (a) non-biotinylated and (b) 5′-biotinylated TMR-labeled 18-base oligonucleotide ((TTAGGG)$_3$) on such a surface are shown. Non-biotinylated DNA adsorbs non-specifically, yielding only isolated, well-separated individual spots (a), whereas biotinylated DNA adsorbs very densely, so that individual spots cannot be resolved (b).

investigated the two main aspects of this approach: the control of streptavidin adsorption onto PEG-coated surfaces (obtained by tuning the amount of biotinylated PEG used during PEGylation), and the specificity of DNA attachment to PEG–streptavidin surfaces.

First, we found that the density of streptavidin can be accurately controlled by tuning the ratio between biotinylated and non-biotinylated PEG used during PEGylation (figures 2(a)–(d)). Due to the repulsive character of PEG surfaces, the measured streptavidin density is almost null if pure non-biotinylated PEG is used (figure 2(a)). Conversely, the use of large fractions of biotinylated PEG (up to 33%) during the PEGylation process results in highly dense coverage of surfaces with streptavidin (figure 2(d)). At intermediate concentrations, the density approximately scales as the ratio of biotinylated PEG used during the PEGylation process (figures 2(b) and (c)). This property is a particularly attractive advantage of PEG coating since the optimal density of immobilized biomolecules depends on the intended application. As demonstrated, purely biotinylated PEG ensures dense coverage, if desired. However, if the aim is the optical study of individual molecules, one should make sure that the average distance between the molecules exceeds the minimal distance that allows their identification using optical microscopy (given by the Rayleigh criterion). The use of low ratios of biotinylated versus non-biotinylated PEG can ensure this separation.

We next investigated to what extent a specific attachment of DNA (i.e. an attachment exclusively involving a chemical group present at a well-defined location on the DNA) can

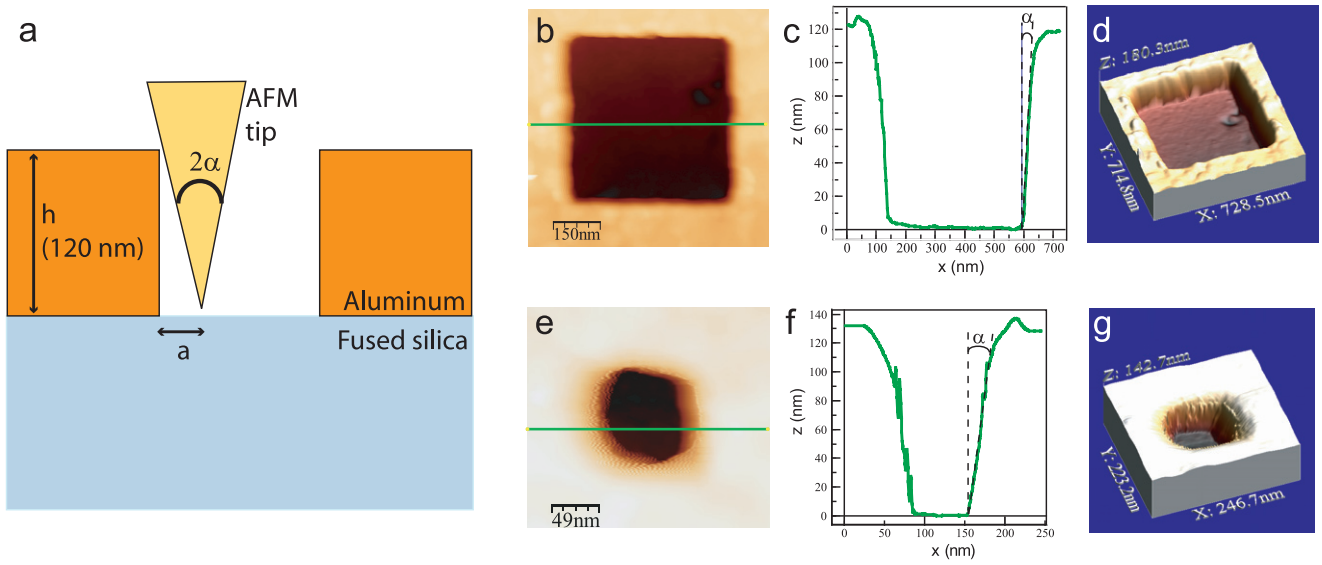

Figure 3. AFM characterization of fabricated waveguides. AFM provides an accurate way to characterize waveguides. As schematically shown in (a), the shape of the AFM tip determines the extent to which it can probe the bottom of waveguides. In particular, given the tip angle of 2α (which has a maximal value of 35° according to the manufacturer), only the region located at a distance greater than $a = h \tan \alpha$ (h being the waveguide depth) from the waveguide walls is accessible to the tip. Therefore, AFM is particularly useful for waveguides of widths larger than $2h \tan \alpha \approx 70$ nm, as their bottom surface can be probed throughout, enabling the measurement of their depth as well as of the roughness of the bottom surface. These measurements provide feedback information on the success of the fabrication process (and on the final etching step in particular). The AFM characterization of a large waveguide, about 500 nm wide, is presented in (b)–(d). (b) 2D image of an individual waveguide. For such sizes, the very square shape which is observed faithfully reproduces the electron beam pattern entered. (c) Height profile corresponding to the green line drawn in (b). This analysis reveals a depth of 120 nm (corresponding to the programed size of the aluminum layer evaporated during the fabrication of this waveguide series). The border of the waveguides displays an apparent slope with an angle $\alpha = 17°$ to the vertical axis, which is compatible with the AFM tip angle provided by the manufacturer (cf (a)). (d) is a 3D representation of the waveguide shown in (b). Figures (e)–(g) are similar pictures obtained with a much smaller waveguide (∼100 nm wide). For such sizes, deviations from a square shape appear (see (e) and (g)), attributable to fabrication. The profile shown in (f) is compatible with a tip half-angle of $\alpha = 14°$.

be achieved. To do so, we incubated bare and biotinylated single-stranded oligonucleotides onto PEG surfaces, and measured the resulting attachment of DNA using fluorescence microscopy. Figures 2(e) and (f) demonstrates that DNA attachment onto our PEG surfaces occurs with high specificity: unlabeled oligonucleotides only weakly adsorb on PEG surfaces (figure 2(e)), whereas high densities of DNA are obtained with the use of biotinylated oligonucleotides (figure 2(f)).

3. Functionalization of nanostructures

Having quantified and optimized the surface conditions on glass slides as described above, we addressed whether these coating protocols could be readily extended to nanostructures. To start, arrays of waveguides were nanofabricated following the approach described in [10]. Briefly, an approximately 100 nm thick aluminum layer was first evaporated onto fused silica slides. Next, a pattern was drawn in the resist using electron beam lithography, which was subsequently revealed using etching (further details are included in the supplementary information (available at stacks.iop.org/Nano/19/465301)). A variant of this approach, based on a negative tone process [16], was also employed for the fabrication of nanostructures with sizes of 100 nm and below. The fabricated nanostructures were then characterized by AFM (figure 3). 'Large' waveguides display a square shape with a size corresponding to that programed into the electron beam pattern generator (an example of a 500 nm wide waveguide is shown in figures 3(b)–(d). 'Small' nanostructures can be successfully fabricated, but typically display larger variations in shape and size (an example of an approximately 100 nm wide waveguide is displayed in figures 3(e) and (f)). Here, too, the AFM is a useful characterization tool, since it can probe the bottom of the waveguides (provided that their aspect ratio exceeds $2 \tan \alpha h$, where α is the half-angle of the AFM tip, typically equal to 35°, and h the waveguide depth). Therefore, AFM provides useful feedback on the fabrication process, as it provides information on the depth of the waveguides and their roughness. For instance, a depth equal to that of the aluminum layer initially evaporated (120 nm for the waveguides displayed in figure 3) and a roughness on the order of one nanometer (figures 3(c) and (f)) indicate a complete etching of the waveguides during the fabrication process.

The PEGylation protocol described above was then applied to these waveguide arrays and the consequences of the coating procedure on the bottom surface of waveguides were investigated by AFM. First, we observed that the roughness of the bottom surface of PEG-coated waveguides displayed an rms roughness of 1–3 nm, similar to that of uncoated

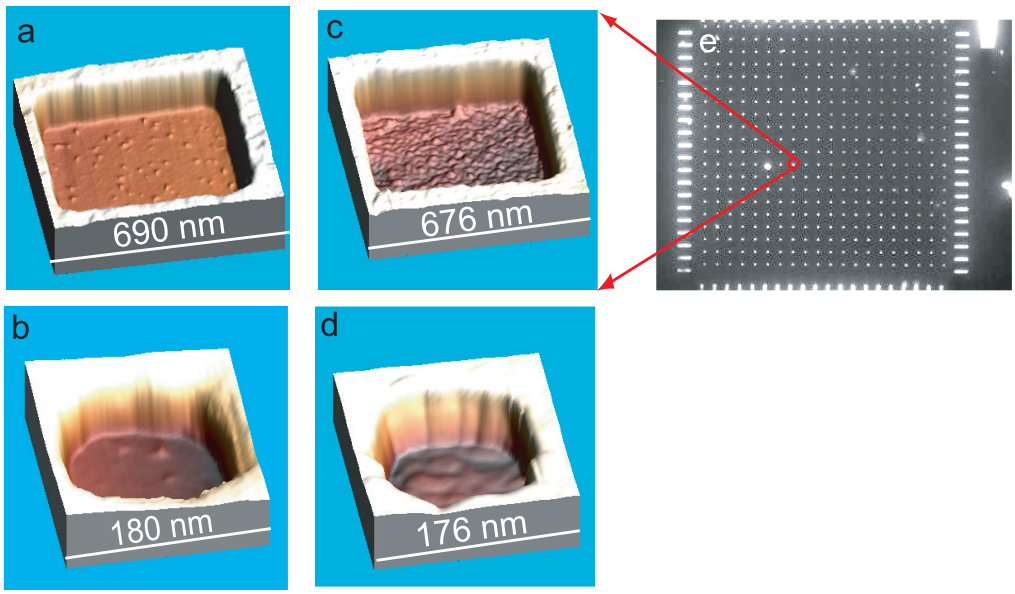

Figure 4. Specific waveguide coating. PEGylation of waveguides proceeds in the same manner as for standard glass slides. Subsequent streptavidin adsorption strongly depends on the biotinylation ratio used during the PEGylation. ((a), (b)) Waveguides coated with 1% biotinylated PEG. (a) shows a relatively large waveguide (about 500 nm wide) whereas (b) illustrates the coating of a smaller structure (about 150 nm wide). Individual streptavidin spots are easily distinguished at the bottom of these two waveguides. ((c), (d)) Waveguides coated with 100% biotinylated PEG. The streptavidin coverage becomes extremely dense, independently of the waveguide width. (e) In this case, a large fluorescence signal is collected from each waveguide of the fabricated array (TMR-labeled streptavidin was used in this study). Waveguides appear as small dots on the picture. Larger, rectangular structures (at the border of the picture) were also fabricated on this slide. Optical measurements are described in supporting information, figure S1 (available at stacks.iop.org/Nano/19/465301).

waveguides (1–2 nm), demonstrating that the PEGylation procedure does not significantly alter the topography of the waveguides. In addition, the adsorption of streptavidin onto the PEG-coated waveguides could also be monitored (figure 4; these experiments can be compared to those on regular glass surfaces described in figure 2). Indeed, individual streptavidin molecules appear as clear spots on the AFM images (shown in a three-dimensional display in figure 4). Figure 4 presents observations on both 500 nm ((a) and (c)) and 100 nm ((b) and (d)) wide nanostructures: in both cases, streptavidin is seen to adsorb within the waveguides. We note that the resulting density of streptavidin molecules strongly depends on the amount of biotin used during waveguide PEGylation (compare (a) with (c), and (b) with (d)). This observation provides evidence for the successful transfer of the PEGylation protocol in nanostructures.

Interestingly, we have noticed that PEG coating is not only effective on glass and silica, but also on aluminum surfaces (tests were done by monitoring the adsorption of fluorescently labeled streptavidin on bare and PEG-coated, semi-transparent, 10 nm thick aluminum films evaporated on glass slides), presumably because of the formation of an oxidized layer at the aluminum–air interface. This finding implies that the coating affects not only the bottom surface of the waveguides, but also all the aluminum surfaces, including the nanostructure walls and the regions between nanostructures. Therefore, the PEGylation of aluminum avoids the massive non-specific adsorption of biomolecules outside the waveguides during subsequent kinetic experiments, without requiring a supplementary surface treatment. However, we note that, in this approach, the biological reaction of interest will take place not only within the waveguides, but also on the aluminum surfaces, therefore mobilizing reagents in optically inaccessible regions. This represents a drawback if the available amount of reagents is limited. However, if desired, this can be circumvented using an alternative protocol based on the selective passivation of aluminum using polyvinylphosphonic acid chemistry, which has been recently described [17]. The use of phosphonic acid in this work was motivated by previous studies which had shown that these acids react with various metal oxides (such as aluminum oxide), but not with SiO_2 surfaces [18, 19].

4. DNA polymerization in PEG-coated nanostructures

Having extended the PEGylation protocol to nanostructures, we tested its potential in the context of fluorescence-based studies of DNA polymerization. Specifically, we tested for successful polymerization on DNA molecules tethered inside nanostructures. Suitable templates for the action of DNA polymerases were produced by annealing a 75-base, biotinylated oligonucleotide with a 14-base complementary oligonucleotide (both from Biolegio). The conversion of this template into a double-stranded product by DNA polymerases in the presence of standard and fluorescently labeled nucleotides was assayed in bulk, using polyacrylamide gel electrophoresis to precisely characterize the reaction products (figure 5). In particular, we found that the

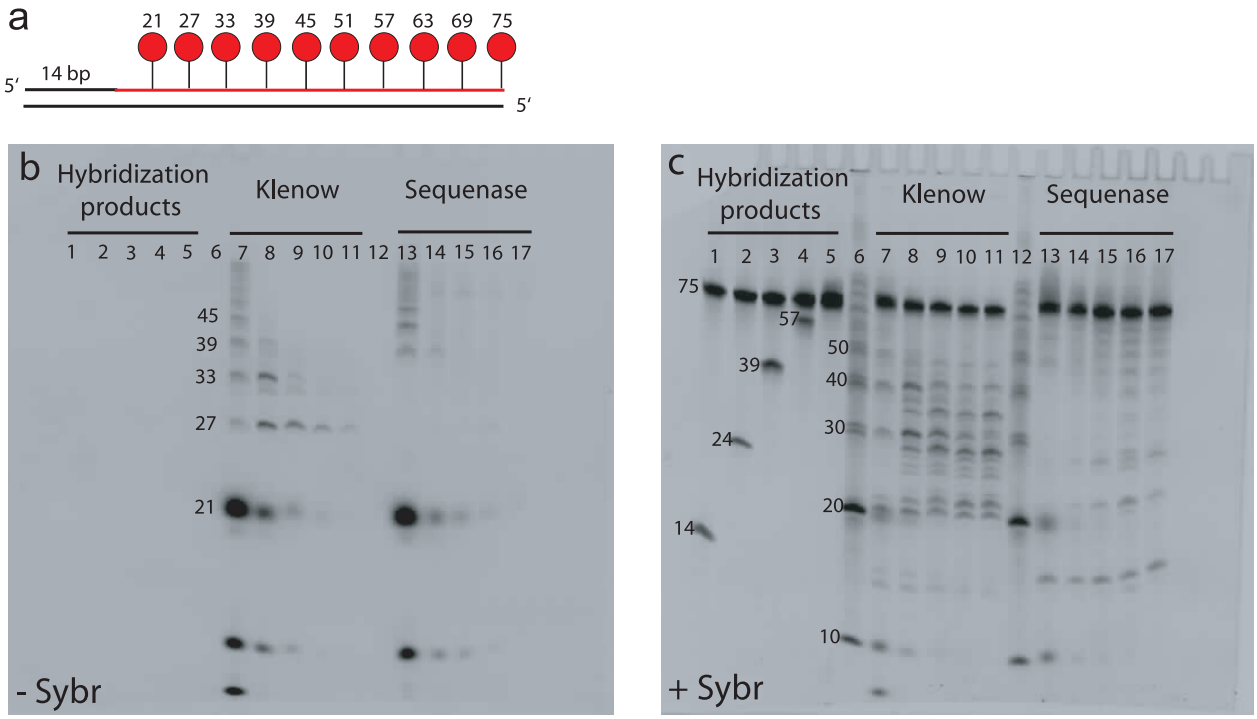

Figure 5. Polymerase: bulk fill-in reaction and detection on a denatured PAGE gel. (a) Experimental strategy. The DNA molecules used during the fill-in reaction are produced by the hybridization of a 75 nt oligonucleotide with a 14 nt complementary oligonucleotide (both shown in black) so as to form a suitable substrate for Klenow and Sequenase polymerases. The sequence to be polymerized is periodic, with one TAMRA-dCTP to be incorporated every six bases (the corresponding positions are shown in red). (b) and (c) show the migration of the products of the fill-in reaction on a 20% denatured PAGE gel. The images were obtained respectively before (b) and after (c) staining of the gel with Sybr Gold: therefore, only fluorescent nucleotides (free or incorporated) are observed in (b), whereas all DNA products become visible in (c). Lanes 1–5 correspond to the migration of the products of various hybridization reactions, in which the 75-base oligonucleotide had been annealed to 14 (1), 24 (2), 39 (3), 57 (4) and 75 (5) bases complementary oligonucleotides. Lanes 6 and 12 are 10 bp DNA ladders (invisible in the unstained gel shown in (b)). The DNA in lanes 7–11 is the result of a fill-in reaction with Klenow polymerase and decreasing concentrations of TAMRA-dCTP: 10 μM (7), 3 μM (8), 1 μM (9), 0.3 μM (10) and 0.1 μM (11), while the products of lanes 13–17 are the result of a reaction carried out with Sequenase and the same decreasing concentrations of TAMRA-dCTP. Note that the brightness of the band at 75 bases in (c) is not meaningful in the context of the fill-in reaction, since this band includes the initial 75-base oligonucleotide of the DNA template.

replacement of standard dCTP with fluorescently labeled dCTP (tetramethylrhodamine-6-dCTP, Perkin-Elmer) in the reaction mixture did not inhibit the polymerization reaction, so that fluorescent products could be generated. However, in agreement with previous reports [20], our gels show that the incorporation of labeled nucleotides is less efficient than that of unlabeled nucleotides. This, together with the possible occasional misincorporation of standard nucleotides in place of labeled ones at high ratios of standard versus labeled nucleotides, was not an obstacle for the present report, which only required the generation of fluorescent products. However, we note that, in the future, these problems should be tackled seriously to extract meaningful kinetic data from real-time experiments.

As a control reaction for polymerase activity on surfaces, the fill-in reaction of surface-anchored DNA templates was first assayed on regular glass. The biotinylated DNA templates were attached on PEG-coated slides, as above (figure 2). Then, the slides were covered with a solution containing polymerases and fluorescently labeled dCTP (at a concentration of 0.1–1 μM) and standard dGTP, dATP and dTTP (1 mM each). After incubation, the slides were extensively rinsed with pure water and dried, so as to remove all unbound molecules. Fluorescence microscopy revealed a large signal (figure 6(a)). However, this observation is not entirely conclusive since the observed fluorescence may have two origins: either the fill-in of fluorescent nucleotides into DNA, or their non-specific adsorption onto the surface. The second possibility can be eliminated by performing a negative control lacking active polymerase: we found that the lack of active polymerase resulted in a dramatic decrease of the fluorescence, with only isolated distinct spots left on the surface (figure 6(b)). Therefore, we conclude that the majority of the fluorescence observed in figure 6(a) results from the incorporation of fluorescent nucleotides into DNA. We carried out similar experiments to demonstrate successful polymerization on DNA molecules tethered in waveguides (figure 7). Here, too, a dramatic difference was observed depending on whether active polymerase had been included or not in the reaction mix. As expected, virtually no fluorescence was seen in the negative control (figure 7(b)). Moreover, we observed a clear transmission of light through the 500 nm wide waveguides used in this negative control (figure 7(d)), attesting to the actual presence of these waveguides. Therefore, we

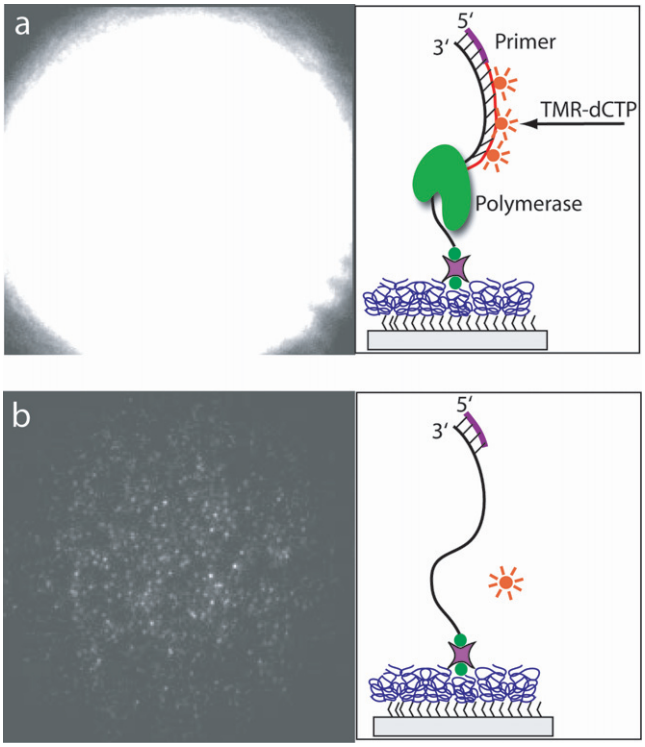

Figure 6. Fill-in reaction on anchored DNA molecules. DNA that is specifically attached to a PEG surface (20% w/v non-biotinylated PEG and 1% w/v biotinylated PEG) constitutes a suitable substrate for Klenow polymerase. Indeed, when Klenow polymerase is incubated with a DNA molecule with an appropriate primer in presence of fluorescently labeled dCTP and unlabeled dATP, dGTP and dTTP, a large fluorescence signal is observed after the complete rinsing of the PEG slide (a). This signal is attributed to the combination of the incorporation of labeled nucleotides along the DNA molecules anchored on the PEG slide and of the non-specific adsorption of fluorescence nucleotides on the surface. To quantify the contribution made by this latter process under the conditions of the fill-in reaction, a negative test is performed without polymerase. Individual spots can then be resolved (b), showing that the largest fraction of the fluorescence observed in (a) comes from the incorporation of fluorescent nucleotides into the DNA.

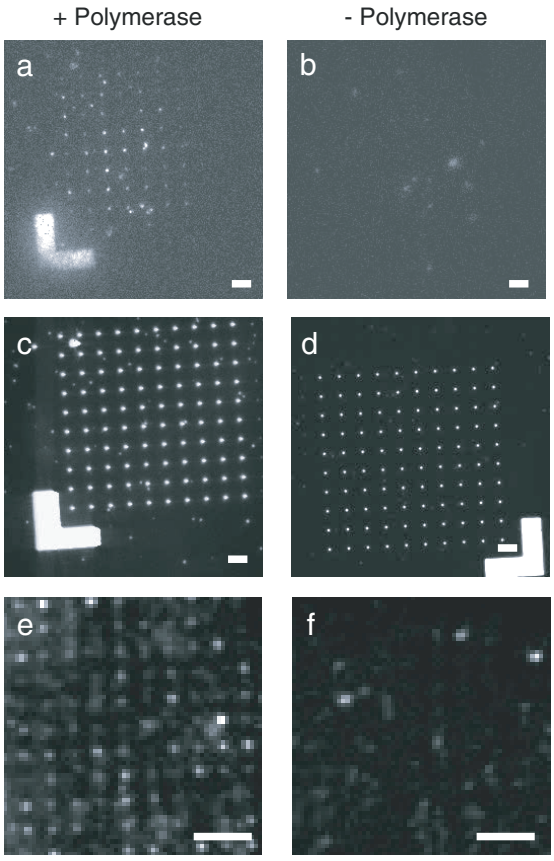

Figure 7. Polymerase: reaction on anchored DNA within waveguides. Waveguide arrays were successively coated with PEG (PEGylation performed with 20% w/v non-biotinylated PEG and 1% w/v biotinylated PEG), streptavidin and biotinylated DNA molecules. A solution containing (left) or lacking (right) Klenow polymerase was introduced within the waveguides. At the end of the reaction, the waveguide samples were rinsed and dried. (a) and (b) show results obtained with 500 nm wide nanostructures. Illumination of the waveguide array with a laser beam generated fluorescence only in the waveguides where active polymerase had been present (a). The actual presence of such large nanostructures can be verified by transmission of white light ((c) and (d), same regions as in (a) and (b)). These images confirm that the absence of fluorescence in (b) is attributable to the absence of polymerase during the reaction and not to a lack of 500 nm wide waveguides. (e) and (f): same as (a) and (b), but with smaller waveguides (nominal size: 80 nm), which optically behave as 'zero-mode waveguides', i.e. do not significantly transmit light. Fluorescence is observed in the majority of waveguides in (e), but not in the negative control (f), in which only defects are apparent. Note that the spacing between waveguides is smaller in (e) and (f) than in (a)–(d) (1.6 μm versus 5 μm). Scale bar: 5 μm. A schematic description of these measurements can be found in the supplementary information (supporting information, figure S1 (available at stacks.iop.org/Nano/19/465301)).

concluded that the absence of fluorescence was attributable to the lack of polymerase, and not to imperfect nanostructure fabrication. Conversely, a clear array of fluorescent spots was observed when active polymerase was included (figure 7(a)). These spots were found to coincide with the position of the waveguides (figure 7(c)). We therefore conclude that fluorescent nucleotides had been successfully incorporated into the surface-anchored DNA molecules present inside the waveguides. Importantly, similar results were obtained for fluorescence experiments involving smaller, 80 nm wide nanostructures (figures 7(e) and (f)), which demonstrates the possibility to run polymerization reactions on DNA molecules attached in zero-mode waveguides.

5. Conclusion

We have shown that PEG coating meets the strict requirements of single-molecule, fluorescence-based studies of polymerization, and that it can be applied to nanostructures. We have demonstrated that polymerization can occur within nanostructures coated with PEG. Although the use of PEG for coating nanostructures is certainly not the only possible choice, it is nonetheless a choice that should be generally favorable since its repellence properties originate from steric hindrance. It thus constitutes a more universal strategy than other coatings based for instance on the use of polyelectrolytes, which rely on

electrostatic interactions and are therefore very sensitive to the charge of the biomolecules used. We have also demonstrated the utility of the AFM for the characterization of PEG-coated surfaces, as it not only provides information about their structure (figure 1), but also allows one to directly monitor the specific and non-specific adsorption of proteins on lengthscales that are inaccessible to optical microscopy (figures 1 and 2). In particular, the possibility to probe the bottom surface of waveguides provides valuable information on both the fabrication process (size and shape of waveguides, as well as the degree of completion of the etching procedure, figure 3) and the surface properties (the adsorption of individual proteins on the bottom surface can be observed, figure 4).

We note that our experimental strategy presents a major difference compared with that used in the works of Levene *et al* [10] and Korlach *et al* [17]. In the aforementioned studies, polymerases were non-specifically adsorbed in waveguides, while DNA molecules were free to diffuse. In contrast, we made the choice to immobilize DNA molecules while maintaining enzymes in solution. An advantage is that DNA binding is highly specific in our case (see figure 2), while, as mentioned by Korlach *et al* [17], the immobilization of polymerases by a non-specific scheme may sometimes alter their biological activity. In addition, the relative advantages of enzyme versus DNA immobilization strategies depend on the processivity of the enzyme under study. Our approach based on DNA immobilization is very suitable for the study of weakly processive enzymes, as it makes it possible to observe the progressive extension of an individual DNA molecule through successive short elongation events. It has the disadvantage, however, of being template limited: the completion of the polymerization of the DNA molecule(s) initially present within a waveguide terminates the experiments. In contrast, a scheme based on surface adsorption of the enzyme under study makes it possible to observe the polymerization of multiple DNA molecules, which could be an advantage when highly processive enzymes are studied.

Finally, the extension of our work to real-time measurements will be a fascinating perspective. The use of gamma-phosphate nucleotides, which lose their fluorescent label once a subsequent nucleotide has been incorporated into DNA, may constitute a good strategy for real-time studies [15], provided that the incorporation time of these nucleotides is long enough to allow for their unambiguous optical detection. Finally, our strategy may allow for kinetic studies involving not only standard DNA polymerases, but also enzymes of great biological importance such as reverse transcriptases and telomerases.

Acknowledgments

We thank Susan Hardin (Visigen, Inc.) for the generous gift of gamma-phosphate-labeled nucleotides and Michael Stone for kindly sending us an initial PEGylation protocol. We also thank Jose Moran-Mirabal for helpful discussions and Marco van der Krogt and Marc Zuiddam from the DIMES facility for technical support. This work was supported by grants from the Netherlands Organisation for Scientific Research and from the European Science Foundation to NHD.

References

[1] Wang M D, Schnitzer M J, Yin H, Landick R, Gelles J and Block S M 1998 *Science* **292** 902
[2] Harada Y, Funatsu T, Murakami K, Nonoyama Y, Ishiahama A and Yanagida T 1999 *Biophys. J.* **76** 709
[3] Wuite G J, Smith S B, Young M, Keller D and Bustamante C 2000 *Nature* **404** 103
[4] Braslavsky I, Hebert B, Kartalov E and Quake S R 2003 *Proc. Natl Acad. Sci. USA* **100** 3960
[5] Revyakin A, Liu C Y, Ebright R H and Strick T R 2006 *Science* **314** 1139
[6] Greenleaf W J and Block S M 2006 *Science* **313** 801
[7] Schomburg D and Schomburg I 2001 *Springer Handbook of Enzymes* (New York: Springer)
[8] Betzig E and Trautman J K 1992 *Science* **257** 189
[9] Betzig E and Chichester R J 1993 *Science* **262** 1422
[10] Levene M J, Korlach J, Turner S W, Foquet M, Craighead H G and Webb W W 2003 *Science* **299** 682
[11] Levene M J, Korlach J, Turner S W, Craighead H G and Webb W W 2005 *US Patent Specification* 6,917,726
[12] Cuvelier D, Rossier O, Bassereau P and Nassoy P 2003 *Eur. Biophys. J.* **32** 342
[13] Ha T, Rasnik I, Cheng W, Babcok H P, Gauss G, Lohman T M and Chu S 2002 *Nature* **419** 638
[14] Rasnik I, McKinney S A and Ha T 2005 *Acc. Chem. Res.* **38** 542
[15] Chan E Y 2005 *Mutat. Res.* **573** 13
[16] Foquet M, Samiee K T, Kong X X, Chauduri B P, Lundquist P M, Turner S W, Fraudenthal J and Roitman D B 2008 *J. Appl. Phys.* **103** 034301
[17] Korlach J, Marks P J, Cicero R L, Murphy D L, Roitman D B, Pham T T, Otto G A, Foquet M and Turner S W 2008 *Proc. Natl Acad. Sci. USA* **105** 1176
[18] Michel R, Lussi J W, Csucs G, Reviakine I, Danuser G, Ketterer B, Hubbell J A, Textor M and Spencer N D 2002 *Langmuir* **18** 3281
[19] Mutin P H, Lafond V, Popa A F, Granier M, Markey L and Dereux A 2004 *Chem. Mater.* **16** 5670
[20] Lacenere C J, Garg N K, Stolz B M and Quake S R 2006 *Nucleosides, Nucleotides & Nucleic Acids* **25** 9